

## Growth and luminescence of elongated In<sub>2</sub>O<sub>3</sub> micro- and nanostructures in thermally treated InN

D. Alina Magdas, Ana Cremades, and Javier Piqueras

Citation: *Appl. Phys. Lett.* **88**, 113107 (2006); doi: 10.1063/1.2185833

View online: <http://dx.doi.org/10.1063/1.2185833>

View Table of Contents: <http://apl.aip.org/resource/1/APPLAB/v88/i11>

Published by the [American Institute of Physics](http://www.aip.org).

---

### Additional information on *Appl. Phys. Lett.*

Journal Homepage: <http://apl.aip.org/>

Journal Information: [http://apl.aip.org/about/about\\_the\\_journal](http://apl.aip.org/about/about_the_journal)

Top downloads: [http://apl.aip.org/features/most\\_downloaded](http://apl.aip.org/features/most_downloaded)

Information for Authors: <http://apl.aip.org/authors>

## ADVERTISEMENT



**Goodfellow**  
metals • ceramics • polymers • composites  
70,000 products  
450 different materials  
**small quantities fast**

[www.goodfellowusa.com](http://www.goodfellowusa.com)

## Growth and luminescence of elongated $\text{In}_2\text{O}_3$ micro- and nanostructures in thermally treated InN

D. Alina Magdas,<sup>a)</sup> Ana Cremades, and Javier Piqueras<sup>b)</sup>

*Departamento de Física de Materiales, Facultad de Ciencias Físicas, Universidad Complutense de Madrid, 28040 Madrid, Spain*

(Received 27 October 2005; accepted 16 January 2006; published online 15 March 2006)

Indium oxide elongated micro- and nanostructures have been grown by thermal treatment of InN powder. Chains of nanopyramids connected by nanowires, forming a necklace-like structure, as well as cubes and arrow-like structures consisting of a long rod with a micron size pyramid on the top, grow at temperatures in the range 600–700 °C in a catalyst free process. The structures have been characterized by scanning electron microscopy and cathodoluminescence. © 2006 American Institute of Physics. [DOI: 10.1063/1.2185833]

Indium oxide is a wide band gap semiconductor with applications in optoelectronics, optical transparency or gas sensing. There is an increasing interest in the synthesis and properties of low-dimensional structures of  $\text{In}_2\text{O}_3$  which have been fabricated by different methods. Pan, Dai, and Wang<sup>1</sup> and Kong and Wang<sup>2</sup> obtained  $\text{In}_2\text{O}_3$  nanobelts by evaporation of powders of the oxide.  $\text{In}_2\text{O}_3$  nanowires have been grown by a thermal evaporation oxidation method with a catalyst<sup>3</sup> by laser ablation<sup>4</sup> or by thermal evaporation of indium and deposition on a substrate.<sup>5–7</sup> In the present work,  $\text{In}_2\text{O}_3$  elongated micro- and nanostructures have been grown by thermal treatment of compacted InN powder under argon flow. This method has been previously reported to lead to the growth of elongated nanostructures, of different semiconductor oxides<sup>8–11</sup> and of CdSe<sup>12</sup> on the surface of the sample so that neither catalyst nor a foreign substrate is used. The obtained structures have been characterized by x-ray diffraction (XRD), scanning electron microscopy (SEM), x-ray microanalysis in SEM and cathodoluminescence (CL) in SEM.

The starting materials used were  $\text{In}_2\text{O}_3$  powder with 99.997% purity and InN powder with 99.9% purity. Samples of both materials were prepared by compacting powder to form disks of about 7 mm diameter and 2 mm thickness. The samples were then annealed at different temperatures, as described below, under argon flow. XRD measurements were performed in a Philips diffractometer. Secondary electron and CL observations were carried out in a Leica 440 SEM and a Hitachi S2500 SEM. The CL measurements were carried out at liquid nitrogen temperature with a beam energy of 15–20 kV with a Hamamatsu R928 photomultiplier and a Hamamatsu PMA-11 charge coupled device camera. Local x-ray microanalysis of the structures was performed in a JEOL JXA-8900 Superprobe by energy dispersive spectroscopy.

Annealing  $\text{In}_2\text{O}_3$  disks at temperatures up to 1400 °C, contrary to the case of  $\text{SnO}_2$ ,<sup>8</sup>  $\text{Ga}_2\text{O}_3$ ,<sup>9</sup>  $\text{ZnO}$ <sup>10</sup> or  $\text{GeO}_2$ ,<sup>11</sup> does not lead to the growth of elongated nanostructures on the disk surface. In order to grow  $\text{In}_2\text{O}_3$  elongated structures, InN was used, instead of  $\text{In}_2\text{O}_3$ , as starting material. InN has a low thermal stability at temperatures at least above 450 °C

and rapid dissociation above 500 °C has been reported (see the review of Ref. 13). Guo, Kato, and Yoshida<sup>14</sup> investigated the thermal stability of InN films and observed that the compound decomposed to In and  $\text{N}_2$  above 550 °C by desorption of nitrogen. The preparation of oxide by using the corresponding nitride as starting material has been also reported in the case of  $\text{TiO}_2$ , e.g., Ref. 15.

The compacted InN powder was annealed under argon flow either with one or with two temperature step treatments. The single step treatments were carried out at 600 or 700 °C for 10 h. In the two step treatments an annealing at 350 °C was followed by a second one at 600 or 650 °C. Both annealings were carried out for 5 or 10 h. The furnace was not sealed for high vacuum conditions so that a pure argon flow was not used. After the single step treatment at 600 °C, some necklace-like structures, formed by rows of pyramids with sizes of about 500 nm connected by nanowires with diameters of less than 100 nm, as those shown in Fig. 1(a), are observed. The treatment at 700 °C produces dense arrays of necklaces and, in some areas, rods with well formed pyramids on the top [Fig. 1(b)], hereinafter referred to as arrows.

The images show that the structures grown at 600 °C are a preliminary stage of growth of those observed after the 700 °C treatment. Also, the linear density and size of the pyramidal pieces of the necklace structure appear to increase at the high temperature, leading to the formation of the rods and arrows. XRD of the annealed samples shows that they are composed of  $\text{In}_2\text{O}_3$ .

The two step thermal treatments were found to favor the growth of the elongated structures in large areas all over the sample surface. The temperature of the second step and the time of each treatment enabled the influence of the final morphology of the structures. When the second step was performed at 600 °C, the necklaces were distributed over the surface. In particular, when the annealing was carried out for 5 h, the pyramids were connected by nanowires with diameters in the range 80–150 nm (Fig. 2) showing in some cases a large separation between the single pyramids, while after a 10 h treatment a dense distribution of pyramids is obtained.

A second step annealing at 650 °C for 10 h leads to the growth of dense arrays of well formed arrows whose rods have lengths in the range of several tens of microns or even over 100  $\mu\text{m}$  [Fig. 3(a)]. By reducing the time of the 650 °C annealing to 5 h, either networks of rods or arrows whose

<sup>a)</sup>Permanent address: Faculty of Physics, Babes-Bolyai University, 400084 Cluj-Napoca, Romania; electronic mail: amagdas@phys.ubbcluj.ro

<sup>b)</sup>Electronic mail: piqueras@fis.ucm.es

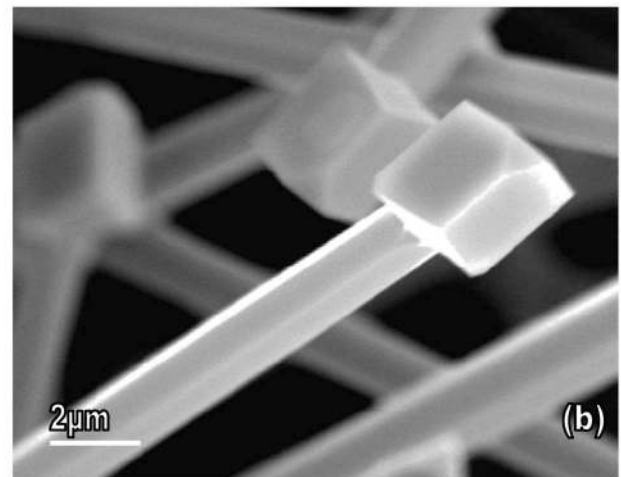
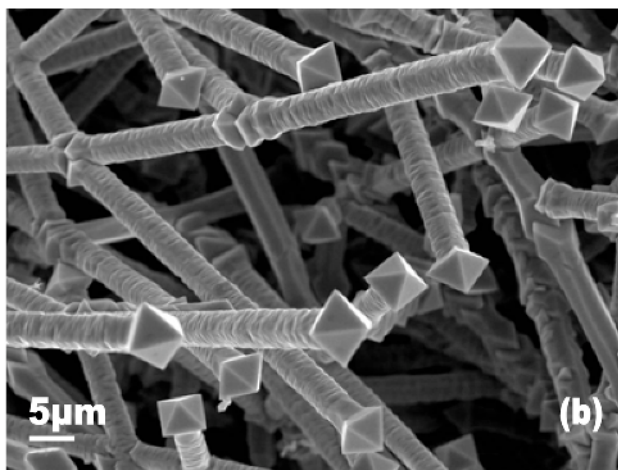
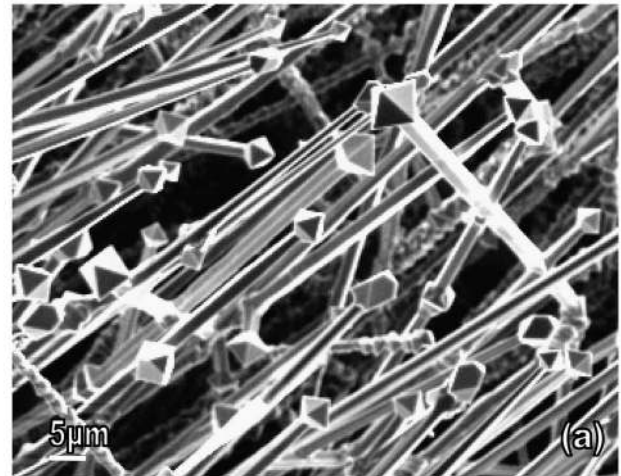
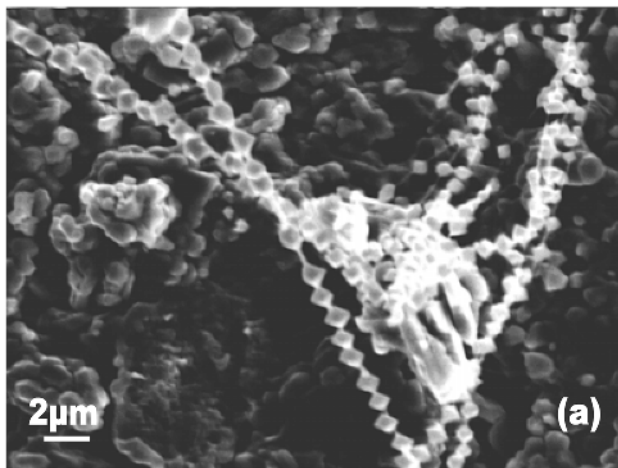


FIG. 3. (a) Arrows and (b) cubes after two step annealing.

FIG. 1. (a) Necklace-like structure in a sample treated at 600 °C, and (b) arrows after treatment at 700 °C.

rods are in an intermediate stage of formation are observed. A reduction of the time of the first step annealing at 350 °C produces a similar structure similar but with a cube at the top [Fig. 3(b)].

The growth of small dimension  $\text{In}_2\text{O}_3$  pyramids has been previously reported. One of the reasons for the interest in such structures is that the sharp tips are useful for efficient field emission<sup>16</sup> having potential applications in displays. Guha, Kar, and Chaudhuri<sup>17</sup> synthesized the pyramids by a

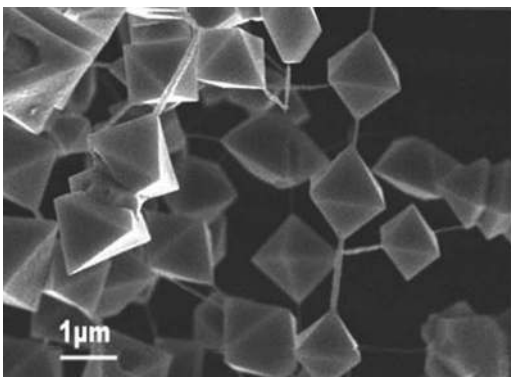


FIG. 2. Pyramids connected by nanowires after a two step annealing with the second step at 600 °C for 5 h.

physical evaporation technique on a silicon substrate. In both works<sup>16,17</sup> the square faces are at the bottom of the pyramids and in contact with the substrate. The pyramids grown in the present work appear in many cases separated from the substrate, which is of potential interest, specially in the case of the arrows, in applications in which single tip field emitters are used. Also the cubes grown in this work appear at the top of a long rod which differs from previously reported  $\text{In}_2\text{O}_3$  nanocubes grown by a hydrothermal method.<sup>18</sup>

Since the starting material in the growth process is InN, compositional analysis of the arrows and other structures has been performed, by x-ray microanalysis in SEM, in order to determine the possible presence of nitrogen. Nitrogen was detected in all cases in amounts ranging from about 0.4 at. % to a maximum of about 9.5 at. % with typical concentrations of a few atomic percent. Comparison of a high number of local composition results reveals that the oxygen atomic content is rather constant, in the range 60%–63%, independent of nitrogen content, while the content of In anticorrelates to that of nitrogen so that the total atomic amount of both elements together is nearly constant in the range 37%–40%. This indicates that nitrogen incorporates in indium sites, with no evidence from XRD measurements of formation of an alloy of the type  $\text{InN-In}_2\text{O}_3$ .

The luminescence from wires, necklaces or arrows appears to be rather homogeneous as observed in the CL image of a region with arrows, shown in Fig. 4.

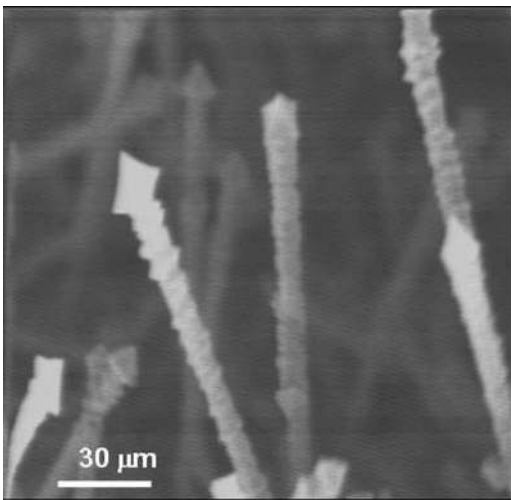


FIG. 4. CL image of arrows.

Figure 5(a) shows the CL spectrum of the commercial untreated  $\text{In}_2\text{O}_3$  powder, with a broadband peaked at about 1.9 eV. A photoluminescence (PL) band at 1.9 eV, observed at room temperature, has been reported in indium oxide polycrystalline films.<sup>19</sup> The PL spectra of Ref. 5 consist of a blue-green band at 2.65 eV in the case of powder and of bands at 2.65 and 3.17 eV in the case of nanowires. The blue-green emission has also been reported in different  $\text{In}_2\text{O}_3$  nanostructures<sup>17,18,20,21</sup> while the PL band peak in the range 3.1–3.2 eV has been observed in nanowires.<sup>7,22</sup>

The CL spectra recorded in the samples treated with the second step annealing at 650 °C are similar to that shown in Fig. 5 [spectrum (a)], with a single broadband peak at about 1.9 eV. It appears that well formed pyramids and rods do not influence the shape of the spectra. In the samples treated with the second step annealing at the lower temperature of 600 °C, luminescence bands at higher energy are observed. A Gaussian deconvolution of the CL spectrum after a second step annealing at 600 °C for 5 h indicates the existence of

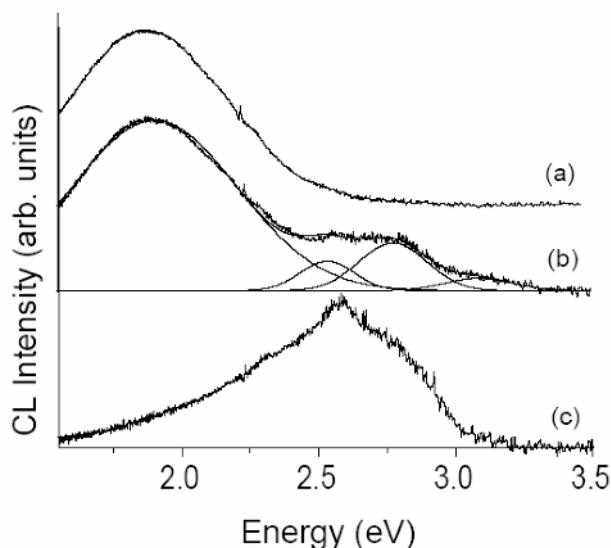


FIG. 5. CL spectrum of untreated  $\text{In}_2\text{O}_3$  powder (a) and CL spectra of a sample after two step annealing in a region with arrows (b) and from a region with necklaces or other structures in an intermediate stage of growth (c).

emissions at 1.90, 2.53, 2.77, and 3.10 eV, as shown in spectrum (b) of Fig. 5. The spectra recorded after 10 h annealing were found to depend on the area considered. In particular, the presence of necklaces seems to favor the blue-green emission at 2.5–2.6 eV [spectrum (c)] while in areas with arrows the spectra are similar to that shown in spectrum (b).

It appears that the blue-green and the 3.1 eV bands are enhanced by the presence of structures in a preliminary stage of growth, as necklaces or arrows with not well formed rods. The blue-green band has been attributed to oxygen vacancies<sup>5,17,18,21</sup> and the 3.1 eV to near band edge emission<sup>22</sup> and to defects generated during growth.<sup>7</sup> The CL results indicate that the samples treated with a second step at 600 °C, contain a higher amount of defects related to oxygen vacancies than those treated at 650 °C, which exhibit well formed structures.

In summary, thermal treatment of compacted InN powder at temperatures in the range 600–700 °C under gas flow causes decomposition of the nitride and formation of elongated  $\text{In}_2\text{O}_3$  micro- and nanostructures with shapes of pyramids, rows of pyramids with a necklace-like morphology, rods and cubes. In the final stage of growth, well formed arrow structures are observed. CL spectra of the samples consist of a broadband centered at about 1.9 eV. In samples with structures in an intermediate stage of growth, a band in the blue-green range, at about 2.6 eV, and a weak emission at about 3.1 eV are observed, which are attributed to oxygen deficiency.

This work has been supported by EU Marie Curie program (HPMT-CT-2001-00215) by MEC (Project No. MAT-2003-00455) and by CAM (Project No. GR/MAT 630-04). D.A.M acknowledges the Marie Curie fellowship in the frame of the HPMT-CT-2001-00215 project.

<sup>1</sup>Z. W. Pan, Z. R. Dai, and Z. L. Wang, *Science* **291**, 1947 (2001).

<sup>2</sup>X. Y. Kong and Z. L. Wang, *Solid State Commun.* **128**, 1 (2003).

<sup>3</sup>C. Liang, G. Meng, Y. Lei, F. Philipp, and L. Zhang, *Adv. Mater. (Weinheim, Ger.)* **13**, 1330 (2001).

<sup>4</sup>C. Li, D. Zhang, S. Han, X. Liu, T. Tang, and C. Zhou, *Adv. Mater. (Weinheim, Ger.)* **15**, 143 (2003).

<sup>5</sup>L. Dai, X. L. Chen, J. K. Jian, M. He, T. Zhou, and B. Q. Hu, *Appl. Phys. A* **75**, 687 (2002).

<sup>6</sup>X. S. Peng, Y. W. Wang, J. Zhang, X. F. Wang, L. X. Zhao, G. W. Meng, and L. D. Zhang, *Appl. Phys. A* **74**, 437 (2002).

<sup>7</sup>F. Zeng, X. Zhang, J. Wang, L. Wang, and L. Zhang, *Nanotechnology* **15**, 596 (2004).

<sup>8</sup>D. Maestre, A. Cremades, and J. Piqueras, *J. Appl. Phys.* **97**, 044316 (2005).

<sup>9</sup>E. Nogales, B. Méndez, and J. Piqueras, *Appl. Phys. Lett.* **86**, 113112 (2005).

<sup>10</sup>J. Grym, P. Fernández, and J. Piqueras, *Nanotechnology* **16**, 931 (2005).

<sup>11</sup>P. Hidalgo, B. Méndez, and J. Piqueras, *Nanotechnology* **16**, 2521 (2005).

<sup>12</sup>A. Urbieto, P. Fernández, and J. Piqueras, *Appl. Phys. Lett.* **85**, 5968 (2004).

<sup>13</sup>S. Strite and H. Morkoç, *J. Vac. Sci. Technol. B* **10**, 1237 (1992).

<sup>14</sup>Q. Guo, O. Kato, and A. Yoshida, *J. Appl. Phys.* **73**, 7969 (1993).

<sup>15</sup>S. Oh and T. Ishigaki, *Thin Solid Films* **457**, 186 (2004).

<sup>16</sup>H. Jia, Y. Zhang, X. Chen, J. Shu, X. Luo, Z. Zhang, and D. Yu, *Appl. Phys. Lett.* **82**, 4146 (2003).

<sup>17</sup>P. Guha, S. Kar, and S. Chaudhuri, *Appl. Phys. Lett.* **85**, 3851 (2004).

<sup>18</sup>Q. Tang, W. Zhou, W. Zhang, S. Ou, K. Jiang, W. Yu, and Y. Qian, *Cryst. Growth Des.* **5**, 147 (2005).

<sup>19</sup>M. S. Lee, W. C. Choi, E. K. Kim, C. K. Kim, and S. K. Min, *Thin Solid Films* **279**, 1 (1996).

<sup>20</sup>H. Zhou, W. Cai, and L. Zhang, *Appl. Phys. Lett.* **75**, 495 (1999).

<sup>21</sup>M. J. Zheng, L. D. Zhang, G. H. Li, X. Y. Zhang, and X. F. Wang, *Appl. Phys. Lett.* **79**, 839 (2001).

<sup>22</sup>H. Cao, X. Qiu, Y. Liang, and Q. Zhu, *Appl. Phys. Lett.* **83**, 761 (2003).